Research article

Potential for U sequestration with select minerals and sediments via base treatment

Hilary P. Emerson[a],[*], Silvina Di Pietro[a], Yelena Katsenovich[a], Jim Szecsody[b]

[a] Applied Research Center, Florida International University, 10555 West Flagler Street, Miami, FL 33174, USA
[b] Pacific Northwest National Laboratory, 902 Battelle Blvd, Richland, WA 99354, USA

ABSTRACT

Temporary base treatment is a potential remediation technique for heavy metals through adsorption, precipitation, and co-precipitation with minerals. Manipulation of pH with ammonia gas injection may be especially useful for vadose zone environments as it does not require addition of liquids that would increase the flux towards groundwater. In this research, we conducted laboratory batch experiments to evaluate the changes in uranium mobility and mineral dissolution with base treatments including sodium hydroxide, ammonium hydroxide, and ammonia gas. Our data show that partitioning of uranium to the solid phase increases by several orders of magnitude following base treatment in the presence of different minerals and natural sediments from the Hanford site. The presence of dissolved calcium and carbonate play an important role in precipitation and co-precipitation of uranium at elevated pH. In addition, significant incongruent dissolution of bulk mineral phases occurs and likely leads to precipitation of secondary mineral phases. These secondary phases may remove uranium via adsorption, precipitation, and co-precipitation processes and may coat uranium phases with low solubility minerals as the pH returns to natural conditions.

1. Introduction

Base injection via ammonia gas is a potential remediation technology for heavy metals including uranium (U). Gas injection has been previously described as a viable remediation technique for heavy metals and radionuclides via pH manipulation as they are highly affected by solution chemistry (Denham and Looney, 2005; Dresel et al., 2011). The injection of ammonia gas is designed to temporarily raise the pH of the aqueous phase to dissolve some natural minerals. When the system returns to a neutral pH as ammonia dissipates from the system, U is expected to be immobilized via the following phenomena (1) adsorption to mineral phases, (2) precipitation of U phases, and (3) co-precipitation as the aqueous phase is saturated with Si, Al, and similar ions followed by (4) coating of adsorbed and (co)precipitated U phases with low solubility precipitates.

The Department of Energy's (DOE) Hanford site located in Washington state represents an ideal case study for this technique as over 200,000 kg of uranium (U) have been released into its deep vadose zone (Corbin et al., 2005; McKinley et al., 2007). This release occurred as a result of improper disposal of waste from plutonium production during World War II and the Cold War. Moreover, U is highly mobile in the Hanford vadose zone due to oxidizing conditions and the presence

of carbonate creating aqueous uranyl ($U(VI)O_2^{2+}$) carbonate species. Partitioning coefficients, K_d's, for U were previously measured in the range of 0.1–5 mL/g at pH 8 and retardation factors were measured at 1.43 for Hanford sediments and groundwater (Szecsody et al., 2013; Zachara et al., 2007). U concentrations have been measured as high as 660 mg/L in groundwater in this area making it one of the primary risk drivers at the site (Serne et al., 2004, 2008; Zachara et al., 2007).

Further, the Hanford vadose zone is up to 255 feet thick with contamination measured down to 170 feet below the ground surface (Serne et al., 2008). Therefore, there is a desire to create a remediation option that does not input additional liquid to the vadose zone as this would increase U flux towards the groundwater below. Of the remediation methods that the Department of Energy (DOE) is currently considering, ammonia gas injection is a favorable option that requires greater investigation. This potential treatment could also be applicable to other sites especially those with vadose zone contamination of heavy metals and radionuclides.

Based on preliminary laboratory-scale column experiments with Hanford sediments, the system may reach a pH of 11–13 depending on the amount of gas injection and will remain elevated for six months or more unless additional gases (e.g. air or CO_2) are injected after ammonia (Szecsody et al., 2010, 2012). For example, the pH was

---

approximately 9.5 after three months in column experiments conducted previously (Szecsody et al., 2010). Therefore, it is imperative that we understand the changes to the aqueous and solid phases caused by mineral dissolution and precipitation with treatment. Some comparisons may be drawn with previous work characterizing vadose zone minerals impacted by highly basic (NaOH and $NaNO_3$ at pH > 13) tank wastes and laboratory column experiments investigating mineral dissolution following ammonia gas treatment. For example, silicates, feldspars, and micas are suggested to be the major dissolving phases in Hanford sediments under highly alkaline conditions based on previous work (Qafoku et al., 2003a; Szecsody et al., 2010, 2012; Wan et al., 2004).

Dissolution of minerals following gas treatment leads to an increase in aqueous Si^{4+} and Al^{3+} as well as small increases in Na^+, K^+, $Fe^{2+/3+}$, Cl^-, F^- and SO_4^{2-} (Szecsody et al., 2012, 2013). Over time, the aqueous phase becomes saturated with respect to several different mineral phases. Some low solubility precipitates that are expected to form based on previous work with tank wastes and vadose zone sediments include cancrinite, sodalite, hydrobiotite, brucite, and goethite (Bickmore et al., 2001; Mashal et al., 2004; Qafoku et al., 2004; Qafoku and Icenhower, 2008; Zhao et al., 2004). Quartz was also demonstrated previously to dissolve and form the following secondary precipitates: brucite, calcite, cancrinite, and portlandite (Zheng et al., 2008). Mashal and team further reported nitrate-cancrinite and sodalite formation due to mineral dissolution and secondary product formation following reaction of Hanford sediments with basic simulated tank waste solutions (pH > 14) (Mashal et al., 2004).

Measurements of the Hanford site's 300 Area Process Ponds has reported extremely slow rates of U adsorption and desorption following interaction with highly basic aqueous waste which has been hypothesized to be due to the creation of unique microporous domains following exposure to pH extremes from waste streams (Zachara et al., 2007). Wan and team also reported that this net precipitation of solids may decrease porosity and permeability of sediments leading to a decrease in U desorption with time (Tokunaga et al., 2004). Szecsody *et al.* reported that as much as 93% less U mass may be leached with 5% ammonia gas injection versus untreated sediments after 100 pore volumes in column experiments with contaminated sediments from the Hanford 200 area (Szecsody et al., 2010). Similar work by Zhong *et al.* reported that 85% less U is mobilized for columns treated with 5 and 15% v/v ammonia gas (Zhong et al., 2015). Nonetheless, there is a lack of understanding of the dominant processes controlling the fate of U and the major precipitates forming under the transient conditions caused by ammonia gas injection. Further, for this technology to be effective for remediation of U, it is important to demonstrate enhanced removal of U from the aqueous phase for a variety of conditions with a decreased release of U in the long-term.

In order to understand the dominant processes, it is necessary to design controlled, laboratory-scale experiments with a well-defined U source term. Szecsody *et al.* have shown that U release from field-contaminated sediments decreased with ammonia gas treatment and that the hard-to-extract U phases (8 M HNO_3 extraction solution) increased following treatment (Szecsody et al., 2010). Research also indicates that U initially in the solid phase associated with carbonates and boltwoodites is not significantly altered with treatment (Szecsody et al., 2012). However, the effect of ammonia gas treatment on U initially in the aqueous phase is still unknown. Enhancement of U removal from the aqueous phase with ammonia gas injection must be confirmed under controlled conditions and associated solid phases must be identified to demonstrate the long-term success of this remediation process. The objective of this work is to quantify partitioning of U and mineral dissolution caused by injection of ammonia in simplified experiments with relevant minerals and sediments. Further, batch samples were prepared with a baseline (a neutral pH representative of natural conditions) and several base treatments including NaOH, NH_4OH, or NH_3 gas to allow for a comparison of ammonia gas injection with additional base

injection techniques and natural conditions at the Hanford site.

2. Methods and materials

2.1. Materials

The following minerals were chosen for experiments based on the mineralogy of the site as summarized in Table S1 in the *Supplementary Materials* with data from Serne et al. (2008), discussions with PNNL collaborators Drs. Jim Szecsody and Nik Qafoku, and previous work (Qafoku et al., 2004; Szecsody et al., 2010; Zheng et al., 2008; Zhong et al., 2015). However, these minerals are also applicable to potential sites worldwide as they represent some of the most common minerals on the Earth's surface. The minerals chosen for experiments include: quartz (Ottawa Sand Standard passed through 20–30 mesh, Fisher), kaolinite (Alfa Aesar), montmorillonite (SWy-2, Crook County, Wyoming, Clay Minerals Society), illite (Imt-2, Silver Hill, Montana, Clay Minerals Society), muscovite (Ward Scientific, < 2 mm size fraction), calcite (Alfa Aesar, 0.06–0.19″ diameter) and Hanford bulk sediments. Each of these minerals are within the 11 most commonly identified minerals in the Hanford formation and were previously identified as potentially dissolving with base treatment (Szecsody et al., 2010, 2012). Hanford sediment samples were received from Dr. Jim Szecsody at PNNL from the ERDF pit in the 200 Area at a depth of 6.1 meters. Further characterization of this sediment has been published previously (Szecsody et al., 2013). BET surface area measurements were collected for each of the minerals investigated with the exception of calcite and are shown in Table 1. Minerals were washed based on methods outlined in Table 2 prior to batch experiments. However, Hanford sediments, muscovite, and calcite were used as received without a washing procedure.

Two solutions were formulated as background electrolytes for these experiments, (1) a simplified synthetic groundwater (SGW) as described in Table 3 and (2) NaCl solution of similar ionic strength for comparison. The simplified SGW is based on correspondence with Dr. Szecsody and previous measurements (Szecsody et al., 1998) to describe the average groundwater composition of the Hanford site. All salts used to prepare background electrolyte solutions were ACS purity or better.

2.2. Experimental methodology

2.2.1. Batch experimental protocols

Batch experiments were conducted in triplicate at pH 7.5 in the presence of minerals and either synthetic groundwater (Table 3) or NaCl at similar ionic strength (7.2 mM) to represent natural conditions in a subsurface in equilibrium with calcite. Experiments were also conducted at elevated pH to mimic those following base treatment with adjustment via 2.5 M $NaClO_4$ + 0.025 M NaOH, 2.5 M NH_4OH, or 5% NH_3/95% N_2 gas. All samples were initially prepared at pH 7.5 in the presence of 500 ppb U (2.1×10^{-6} M, Spex Certiprep, New Jersey) and background electrolytes as either SGW or NaCl. This initial U concentration is consistent with concentrations of U measured previously at 487 ppb in leaching experiments for contaminated sediments

Table 1
BET surface area for relevant minerals and Hanford sediment.

Mineral ID	m^2/g
Montmorillonite	23.8
Illite	19.1
Kaolinite	17.9
Hanford Sediment	17.4
Muscovite	0.096
Calcite	0.068
Quartz	0.046

Table 2
Summary of Mineral Washing Methods.

Mineral	Method	Reference
Quartz (Ottawa Sand)	(1) Mix 100 g/L suspension in 0.01 M NaOH for 60 min, (2) Centrifuge, decant, replace liquid with 0.01 M HCl, mix 60 min, (3) Centrifuge, decant, replace with Nanopure (> 18 MΩ) H_2O and mix 3 min, (4) repeat step three two more times, (5) Dry solid at 35 °C for ~3 days	(Boggs et al., 2015; Powell et al., 2008; Zavarin et al., 2012)
Montmorillonite	(1) Mix 100 g/L suspension in 0.001 M HCl for 30 min, (2) Add 0.5 mL H_2O_2 and mix an additional 30 min, (3) Centrifuge 6 h at 4500 rpm, decant aqueous and replace with 0.01 M NaCl (or synthetic porewater for synthetic porewater experiments) and mix overnight, (4) Repeat four times, (5) Centrifuge, decant and replace with Nanopure H_2O, (6) Repeat at least four times (until excess ions are removed), (7) Dry solid at 35 °C for ~3 days, (8) Lightly crush with a mortar and pestle to homogenize	(Boggs et al., 2015; Powell et al., 2008; Zavarin et al., 2012)
Kaolinite	(1) Mix 100 g/L suspension in 1 M NaCl (synthetic pore water for synthetic porewater experiments) for 30 min, (2) Centrifuge, decant and repeat four more times, (3) Centrifuge, decant and replace with Nanopure H_2O, (4) repeat four more times, (5) Dry solid at 35 °C for ~3 days, (6) Lightly crush with a mortar and pestle to homogenize	(Heidmann et al., 2005)
Illite	(1) Mix 100 g/L suspension with 1 M NaCl (or synthetic porewater) for three hours and allow to flocculate overnight, (2) Decant and replace with 1 M NaCl (or synthetic porewater) and mix, (3) Repeat two more times, (4) Decant and replace with Nanopure H_2O, (5) Repeat until excess ions are removed, (6) Dry solid at 35 °C for ~3 days, (7) Lightly crush with a mortar and pestle to homogenize	(Baeyens and Bradbury, 2004)

Table 3
Synthetic groundwater (SGW) composition (total ionic strength of 7.2 mM).

Element	(mmol/L)
Na^+	1.1
K^+	0.22
Ca^{2+}	1.4
Mg^{2+}	0.6
HCO_3^-	1.32
Cl^-	3.9

removed from the Hanford 200 Area (Szecsody et al., 2010). Batch experiments were conducted for each of the minerals described in the Materials section at the following concentrations: 100 g/L for quartz, 5 g/L for kaolinite, illite, montmorillonite, and calcite, 25 g/L for muscovite and Hanford 200 Area sediments, and based on sorption affinity at neutral pH and surface area. Then, samples were equilibrated for three days with U on an end-over-end tube revolver at 40 rpm (Thermo Scientific). Upon sampling, a homogenous aliquot was removed for analysis for both controls (without minerals and sediments) and samples in the presence of minerals.

Following equilibration at pH 7.5 and three day sampling, the pH of triplicate samples was raised with either aqueous 2.5 M NH_4OH or 2.5 M $NaClO_4$ + 0.025 M NaOH or exposure to 5% NH_3/95% N_2 gas for approximately 12 h. Samples adjusted with NH_4OH were immediately capped and wrapped with Para film following addition to reduce volatilization of NH_3 gas. It should be noted that ammonia volatilization increases by an order of magnitude for every unit above pH 6.0 and, therefore, is expected to be higher in alkaline soils and conditions (Bouwmeester and Vlek, 1981; Singandhupe and Rajput, 1989). The pH adjust solutions with NaOH and NH_4OH were prepared to allow for similar ionic strength and base adjusting power, i.e. $NaClO_4$ was added to NaOH to account for ionic strength changes in samples. In addition, adjustment by either NH_4OH or NaOH allows for comparison of both options as a possible step to raise the pH during remediation of the subsurface. Samples exposed to ammonia gas were placed inside a glovebag (Glas-Col, Terre Haute, Indiana) filled with 5% NH_3/95% N_2 gas uncapped for approximately 12 h before capping, wrapping with Para film, and removing from the glovebag. Minimal losses of liquid due to evaporation in the bag occurred (< 0.2%). After adjustment, samples were equilibrated for either three days or three weeks before analysis as described in the sampling protocols section for U and major cations.

2.2.2. Sampling protocols
Both pH (Thermo Scientific, 8175BNWP) and redox conditions

(Mettler Toledo, EM40-BNC) were analyzed prior to removal of an aliquot for U and major cation measurement. All samples (except for montmorillonite) were centrifuged at 5000 rpm for 30 min (18100 rcf, Thermo Scientific, Corvall ST 16R centrifuge) to remove particles > 100 nm based on Stoke's law as described by Jackson (1985). Montmorillonite was subjected to a longer centrifugation step for three hours to remove particles > 40 nm due to the greater likelihood of colloid formation based on previous work (e.g. Lagaly and Ziesmer, 2003). The supernatant was acidified in 1% HNO_3 (Fisher, ACS Plus) for analysis by kinetic phosphorescence analyzer (KPA-11, Chemchek) for U and inductively coupled plasma optical emission spectroscopy (ICP-OES, Perkin Elmer Optima 7300 DV) for major cations (Ca, Mg, Na, K, Fe, Al and Si). The cation concentrations in the aqueous phase were analyzed to track dissolution of minerals and losses of SGW components throughout these experiments. The minimum detectable concentration (MDC) for U via KPA is 5 ppb (2.1×10^{-8} M). The MDC for major cations via ICP-OES were: Al 60 ppb, Fe 94 ppb, Ca 94 ppb, Mg 70 ppb, Si 120 ppb, K 115 ppb, and Na 142 ppb.

3. Results and discussion

3.1. Mineral dissolution

Fig. 1 depicts the fraction of Al and Si in the aqueous phase in the presence of SGW and 7.2 mM NaCl for clay minerals per the aforementioned sampling protocols (2.2.2) with the aqueous fraction based
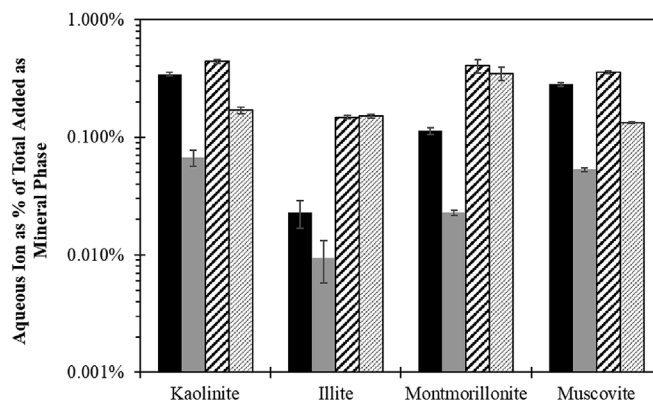

Fig. 1. Aqueous Si (*patterned*) and Al (*solid*) fractions of total mineral added as measured in batch experiments with 5 g/L (kaolinite, illite, and montmorillonite) or 25 g/L (muscovite) in the presence of 7.2 mM NaCl (*black*) or SGW (*gray*) at three days after treatment with 5% NH_3/95% N_2 gas, Note: error bars are based on measurement of triplicate samples.

on each mineral's chemical formula and the initial mineral concentration. Therefore, the cations are present in the aqueous phase due to dissolution of mineral phases. However, because we expect complex dissolution and re-precipitation processes to be ongoing during these experiments, they cannot represent a simple fraction dissolved. Therefore, we will refer to the results as the percent measured in the aqueous phase. The greatest aqueous cation measurements at elevated pH were collected for kaolinite and muscovite minerals. However, the greatest dissolution of any mineral occurred for calcite at neutral pH with 3.5% of Ca^{2+} in the aqueous phase in 7.2 mM NaCl batch experiments. Calcite dissolution was measured similarly to the clay minerals but by monitoring aqueous Ca^{2+}. However, it is not shown in Fig. 1 as these data represent aqueous Si and Al from clay minerals. At elevated pH, only ~0.6% of calcite was measured in the aqueous phase as its solubility theoretically decreases with increasing pH. Moreover, it is likely that secondary minerals were formed at elevated pH in the calcite solutions as there is clear evidence that Ca^{2+} was removed from the aqueous phase with treatment following a three day equilibration period at elevated pH. SGW background solutions were saturated with respect to calcite at elevated pH during treatments as shown by speciation modeling previously (Emerson et al., 2017) and greater than 30% of Ca^{2+} was removed from SGW during base treatments. Quartz is not included in the results as minimal dissolution was measured (<0.1%) throughout experiments based on aqueous Si measurements.

Significant dissolution of minerals occurs within three days of base treatments (up to 0.3%) based on aqueous Al and Si measurements by ICP-OES. Aqueous Al and Si were consistently above detection limits for all clay minerals. Other cations were monitored including Ca, Mg, and Fe and are presented in *Supplementary Materials* Figs. S8–15. These results are consistent with previous research which showed that overall mineral dissolution was rapid in the first 48 h (Qafoku et al., 2003b). Previous research also reported substantial dissolution of the phyllosilicates (montmorillonite, muscovite, and kaolinite) under similar conditions (Szecsody et al., 2012).

A comparison of aqueous Si and Al ratios suggests that incongruent dissolution is occurring in batch experiments. This further shows that the aqueous measurements are not representative of the total percent of minerals dissolved as secondary precipitation often coincides with incongruent dissolution. Similar trends were observed for each base treatment (NH₃ gas, NaOH, and NH₄OH) as shown in *Supplementary Materials* Figs. S12–15. Minor effects of background electrolyte solutions were also observed and are likely due to their influence on secondary mineral formation (i.e. greater precipitation of Al may occur in SGW potentially due to co-precipitation with calcite).

Phases predicted to form by equilibrium thermodynamic speciation modeling include chrysotile, quartz, calcite, dolomite, diaspore and hematite (Szecsody et al., 2012). However, it is likely that intermediate phases form initially. For example, amorphous iron hydroxide species often form first before hematite. Further, these data trend towards incongruent dissolution with greater Si measured in the aqueous phase suggesting formation of secondary Al phases like diaspore and gibbsite. Additional experiments are ongoing to monitor mineral dissolution and re-precipitation processes with time and will be included in a future publication. Mineral dissolution rates may be measured via column experiments in order to avoid secondary precipitation and solid phase characterization is ongoing to identify changes in bulk and surface mineral phases (XRD and FTIR, respectively).

3.2. Uranium removal in the presence of pure minerals at neutral pH

U removal from the aqueous phase is lowest at neutral pH in the SGW solution with the exception of muscovite (Fig. 2) with partitioning coefficients measuring <100 mL/g. Previous XAS work has shown that U removal occurs through surface precipitation on muscovite which may explain the consistent removal of U in the presence of muscovite with varying pH (Moyes et al., 2000). Further, significant removal of U
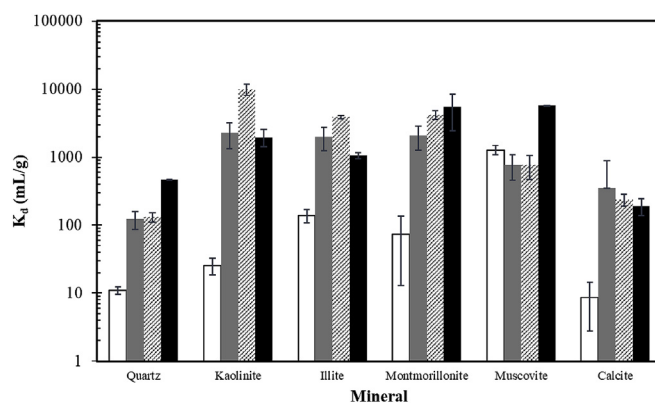

Fig. 2. U [initially 500 ppb] partitioning coefficients (K_d, mL/g) following three days of equilibration at pH 7.5 (initial conditions – *white*) or pH 11.5 (via NaOH – *gray*, NH₄OH – *striped*, or NH₃ gas – *black*) with minerals at 5 g/L (kaolinite, illite, montmorillonite, and calcite) or 25 g/L (muscovite and Hanford sediments) in the presence of synthetic groundwater SGW (7.2 mM ionic strength), Note: error bars are based on triplicate samples.
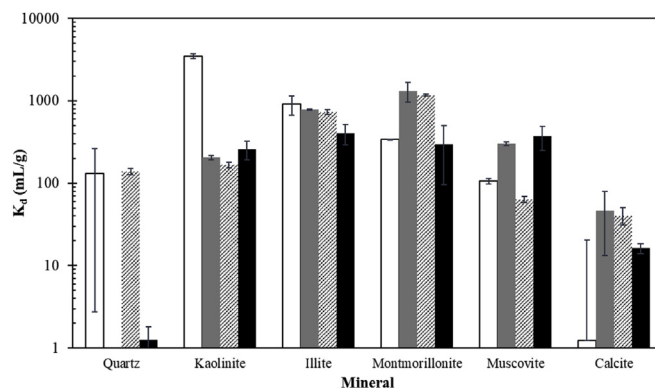

Fig. 3. U [500 ppb] partitioning coefficients (K_d, mL/g) following three days of equilibration at pH 7.5 (initial conditions – *white*) or pH 11.5 (via NaOH – *gray*, NH₄OH – *striped*, or NH₃ gas – *black*) with minerals at 5 g/L (kaolinite, illite, montmorillonite, and calcite) or 25 g/L (muscovite and Hanford sediments) in the presence of 7.2 mM NaCl, Note: error bars are based on triplicate samples.

occurs at neutral pH for each of the minerals in 7.2 mM NaCl (Fig. 3). The significant differences in U adsorption for the two electrolyte solutions are due to changes in aqueous U speciation.

In the presence of SGW, sorption is low at pH 7.5 due to the formation of uranyl carbonate species within the aqueous phase. Fig. S1 in the *Supplementary Materials* predicts neutral and negatively charged complexes [$CaU(CO_3)_3^{-2}$, $Ca_2U(CO_3)_3$, and $(UO_2)_2CO_3(OH)_3^-$] as the major aqueous species based on a Geochemist Workbench (GWB) equilibrium speciation model developed previously (Emerson et al., 2017). These species are not expected to sorb as strongly at neutral pH due to (1) electrostatic repulsion from negatively charged mineral surfaces for negatively charged aqueous species and (2) poor sorption affinity for neutrally charged species. These species are also consistent with the results in Fig. 1 as they have been confirmed to exist at neutral pH and to exhibit decreased surface complexation affinity by previous researchers (Dong and Brooks, 2006; Fox et al., 2006). Moreover, aqueous speciation predictions by GWB are confirmed by previous work to be representative of Hanford site groundwater (Szecsody et al., 2010).

Significantly increased adsorption of U was observed in 7.2 mM NaCl at neutral pH as compared with the SGW solutions. Although uranyl carbonate species are predicted for the NaCl system at neutral pH if equilibrated with air (Fig. S2, *Supplementary Materials*), it is unlikely that these suspensions were open to the atmosphere for a

sufficient period of time to completely equilibrate with atmospheric CO_2. Therefore, without formation of aqueous uranyl carbonate species, significant adsorption of U occurs for the minerals investigated with the exception of calcite. Negligible removal of U from the aqueous phase occurred in NaCl electrolyte equilibrated with calcite at neutral pH. This is likely due to significant dissolution of Ca^{2+} and CO_3^{2-} at neutral pH followed by formation of weakly sorbing, ternary Ca-uranyl-carbonate complexes as identified previously (Dong et al., 2005; Dong and Brooks, 2006). Further, as discussed in section 3.1, aqueous phase measurements of Ca^{2+} by ICP-OES were approximately 50 μM which is consistent with dissolution of calcite at near neutral pH.

Previous research has shown that carbonate minerals are among the most reactive under Earth surface conditions and exhibit relatively significant dissolution in comparison to other minerals (Morse and Arvidson, 2002; Morse and Mackenzie, 1990). Significantly greater error in triplicate measurements was observed in both NaCl and SGW solutions for calcite as compared to other mineral phases. Previous work suggests that this greater error may be due to relatively fast dissolution and re-precipitation processes leading to incorporation of U (Morse and Arvidson, 2002; Morse and Mackenzie, 1990). When surface area is accounted for, removal of U is greatest for quartz and kaolinite for NaCl background solution and quartz and muscovite for SGW solution at neutral pH (*Supplementary Materials*, Fig. S3). Overall, quartz exhibited the greatest removal once surface area was accounted for in partitioning coefficients (units mL/m^2) as has been shown in previous research (Dong et al., 2012). Further, it is notable that removal is greater when compared to surface area for all mineral phases in 7.2 mM NaCl as compared to SGW with the exception of muscovite and Hanford sediment.

3.3. Uranium fate in the presence of pure minerals upon base treatment

Because of the likelihood of co-precipitation processes occurring under basic conditions due to background electrolyte components and mineral dissolution and re-precipitation, batch data presented in Figs. 2–3 represent an apparent K_d and are assumed to include precipitation, co-precipitation, and adsorption processes in the overall partitioning coefficient. Because the base treatments are dissolving minerals, a direct comparison with initial BET surface area measurements cannot be drawn for data at elevated pH. Moreover, it must be noted that co-precipitation is significant in the control samples for SGW at elevated pH due to saturation with respect to calcite further highlighting that there will be multiple, complex reactions occurring in the natural environment. Mineral-free control samples prepared in the absence of minerals and sediments that were analyzed at elevated pH showed considerable losses of U from the aqueous phase for SGW conditions ($\sim$30%). Recovery of U in the aqueous phase in control samples prepared in triplicate for the SGW and 7.2 mM NaCl is presented in *Supplementary Materials* Fig. S4. The fraction of U remaining in the aqueous phase for control samples at neutral pH are nearly 100% (94 ± 10% for SGW and 96 ± 6% for NaCl).

The batch data presented in Figs. 2 and 3 is corrected for control recovery for the initial conditions at pH 7.5 as losses are assumed to be due to sorption to vial walls and/or losses during sampling and pH adjustment. Samples in NaCl background electrolyte are also corrected for control losses for base treatments. However, in SGW controls, the aqueous phase recovery after treatment with ammonia gas to pH 11.5 is significantly decreased. These samples were not corrected for the recovery of U in the controls at elevated pH due to the complexity of the processes occurring in this system. Results and GWB modeling suggest that co-precipitation, precipitation, and adsorption are occurring simultaneously. These removal processes likely occur at different levels in samples with and without minerals. We suggest that removal at elevated pH is primarily due to co-precipitation of U with calcite formed from SGW components and/or precipitation of uranyl silicate minerals as suggested by previous work (Emerson et al., 2017;

Katsenovich et al., 2018; Szecsody et al., 2012). However, in the presence of minerals, it is possible that a decrease in precipitation may occur due to sorption of cations that would otherwise precipitate and remove U. There is also the potential for greater co-precipitation as other mineral phases dissolve at elevated pH and saturate the aqueous phase.

Results presented in Fig. 2 represent measurements after three days of equilibration. However, due to the complex sorption, dissolution, and precipitation processes occurring in these systems at elevated pH, they likely do not represent equilibrium. Therefore, additional analyses were conducted at three weeks (21 days) and are presented in the *Supplementary Materials* Figs. S5–6. These results show that U partitioning coefficients are increasing with reaction time. Future work will consider aging periods up to six months as Szecsody *et al.* has predicted that the pH may remain elevated within the subsurface for six months or more during treatment in a deep vadose zone environment (Szecsody et al., 2010). For experiments at neutral pH, results were similar for variable time samples after three days and are consistent with previous research suggesting that this period is sufficient to reach sorption equilibrium for U (Dong et al., 2012; Emerson et al., 2017).

Removal of U increases significantly with base treatment for each of the minerals investigated in SGW with the exception of muscovite where similar removal is observed for each condition investigated (Figs. 2 and 3). Although it appears that removal increases with ammonia gas treatment as compared to NaOH and NH_4OH, aqueous U measurements were below detection limits for many of these samples (5 ppb U after dilution correction or K_d of 3960 for 25 g/L mineral concentrations and 19800 for 5 g/L mineral concentrations) so statistical differences are unclear. Removal is slightly greater for silicate layer clays (kaolinite, illite, montmorillonite and muscovite) as compared to quartz and calcite likely due to (co)precipitation with ions dissolved or exchanged from clay mineral surfaces.

Calcite samples exhibited increased U removal with basic treatments although lower than other minerals without a significant difference between the treatments (i.e. NaOH versus NH_4OH versus NH_3 gas). These results are consistent with previous work which observed a significant impact of carbonate coatings or co-precipitates on U behavior (Dong et al., 2005). This indicates that precipitation and/or inner-sphere adsorption are also occurring that are increased by the base treatment. Results for the NaCl electrolyte are less conclusive (Fig. 2), but, overall, base treatment significantly enhances U removal in the presence of calcite but is not significantly different between treatments. This result highlights the significant impact of aqueous calcium and carbonates on both adsorption and co-precipitation processes of U due to the lack of both in the NaCl background electrolyte as compared with the SGW. Furthermore, these components are expected to play a significant role in remediation with base injection at the Hanford site as some naturally occurring minerals containing calcium, carbonate, and uranium are already present including betafite ($Ca_{0.92}U_{1.08}[Ti_2O_7]$) and calcite minerals (McKinley et al., 2007; Szecsody et al., 2010).

3.4. Uranium behavior before and after base treatment in the presence of Hanford sediments

For the Hanford sediments, U adsorption was significantly lower than results for clays at neutral pH conditions potentially due to dissolution of carbonates or desorption and ion exchange of competing cations during experiments as these sediments were not washed like pure minerals (Fig. 4). Calcite content is variable at the Hanford site but has been measured as high as 5% in the bulk phase (Serne et al., 2008). Under basic conditions, the removal of U is also the lowest for the Hanford sediments as compared to pure minerals although still increased by more than three orders of magnitude as compared to neutral pH conditions. This implies that there are fewer available sorption sites within the heterogeneous mixture of minerals in the sediments possibly because minerals are coating one another and blocking sorption sites
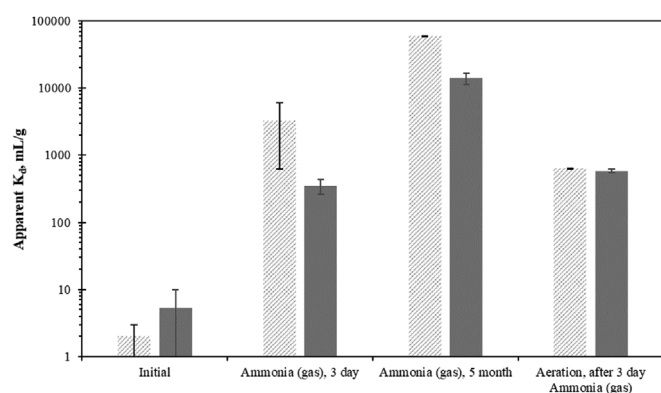
Fig. 4. U apparent partitioning coefficients (K_d, mL/g) in 25 g/L Hanford sediment suspensions in the presence of SGW (*stripes*) or NaCl (*solid*) background solution and variable conditions (initial conditions are pH 7.5 and NaOH, NH_4OH and NH_3 gas treatments are adjusted to pH 11.5), aerated sample bubbled air to remove NH_3 gas for ~48 h after 3-day exposure to NH_3 gas, Note: error bars are based on measurement of triplicate samples.

Table 4
Comparison of average aqueous ORP (mV) for all samples prepared in the presence of variable minerals and background electrolyte solutions under initial conditions (pH 7.5) or at pH 11.5 via treatment with NaOH, NH_4OH, or 5% NH_3/ 95% N_2 gas.

Condition	ORP (mV)
Initial	527 ± 48
NaOH	296 ± 15
NH_4OH	187 ± 28
NH_3	150 ± 15

and/or that less co-precipitation is occurring due to exchange of ions with surface sites.

U removal increases along the trend initial conditions < NaOH < NH_4OH < NH_3 gas. Therefore, it is possible that the different ions associated with the treatments may impact removal of U by blocking or competing for potential adsorption and exchange sites. However, a decrease in oxidation-reduction potential (ORP) in the aqueous phase was also observed following this trend (Table 4 and *Supplementary Materials* Fig. S7). Therefore, it is unclear which mechanism may be controlling U fate, although there are likely multiple factors controlling behavior in this complex system. We hypothesize that decreasing ORP conditions may lead to temporary reduction and precipitation of U.

The lowest aqueous ORP conditions were reached in gas treated samples as carbon dioxide and oxygen will be stripped from the aqueous phase during gas equilibration leading to enhanced adsorption, reduction, and precipitation of U (Table 4). Although, carbonate concentrations were not measured in samples, the oxidation-reduction potential (ORP) is significantly decreased for both NH_4OH and NH_3 treatments with the lowest values measured for the NH_3 gas treatment (Table 4). Another indication that greater precipitation of U may be occurring under the reduced ORP conditions is shown upon comparison of U partitioning coefficients (mL/g) versus ORP (mV) for both background electrolytes, all mineral samples, and conditions as shown in the *Supplementary Materials* Fig. S7 as a clear trend emerges with significantly greater U apparent partitioning coefficients at lower aqueous ORP. Moreover, it is possible that ORP is even lower on the surface of mineral phases. This depiction does not take into account the exact pH of samples or which minerals are present, which is extremely significant, but it shows that below 250 mV removal of U increases dramatically.

This result is consistent with previous work predicting that reduction of uranium may occur below 250 mV (Eh with respect to a SHE) (McKinley et al., 2007). Moreover, the lower redox conditions observed with NH_3 gas treatment, although potentially transient, may explain previous observations of some mixed oxidation (+4 and +6) U precipitates as measured by XANES analysis of the U L_{III} edge for a sediment sample with 690 μg/g of U treated with ammonia gas (Szecsody et al., 2010). Additional work is ongoing to characterize solid phases following variable periods of exposure to ammonia gas to confirm the dominant processes controlling the long-term behavior of U and will be presented in future publications. Fig. 4 also highlights that even following aeration (through bubbling of air) after a three day exposure to NH_3 gas, U apparent partitioning coefficients are still greater than two orders of magnitude higher than natural conditions at neutral pH. These data suggest that U is not readily re-oxidized following treatment potentially due to incorporation into minerals with low solubility at neutral pH.

4. Conclusions

These results highlight the significant impact of base treatment on adsorption, precipitation, and co-precipitation processes. The potential importance of aqueous calcium and carbonates on the removal of U is highlighted via comparison of experiments with either NaCl background electrolyte or SGW. Significant incongruent dissolution of clays occurs at elevated pH suggesting secondary mineral formation which likely also contributes to increases in U removal from the aqueous phase. These components are expected to play a significant role in remediation with base injection at sites similar to Hanford with naturally occurring calcium carbonate minerals, although significant U removal still occurs in NaCl solutions indicating that co-precipitation with carbonates is not the only mechanism for removal. Apparent partitioning coefficients were shown to increase by at least two orders of magnitude following NH_3 gas treatment in SGW including following aeration for batch experiments with Hanford sediments. We suggest that these results provide evidence of future outcomes for pilot and field scale remediation efforts in the Hanford vadose zone as well as other vadose zone environments in equilibrium with calcite minerals and with clays (McKinley et al., 2007; Serne et al., 2008; Wellman et al., 2008). Overall, injection of ammonia gas could increase removal of U from the aqueous phase by more than two orders of magnitude.

Appendix A. Supplementary data

Supplementary data related to this article can be found at http://dx.doi.org/10.1016/j.jenvman.2018.06.012.

References

Baeyens, B., Bradbury, M.H., 2004. Cation exchange capacity measurements on illite using the sodium and cesium isotope dilution technique: effects of the index cation, electrolyte concentration and competition: Modeling. Clay Clay Miner. 52, 421–431.

Bickmore, B.R., Nagy, K.L., Young, J.S., Drexler, J.W., 2001. Nitrate-cancrinite precipitation on quartz sand in simulated Hanford tank solutions. Environ. Sci. Technol. 35, 4481–4486.

Boggs, M.A., Dai, Z., Kersting, A.B., Zavarin, M., 2015. Plutonium(IV) sorption to montmorillonite in the presence of organic matter. J. Environ. Radioact. 141, 90–96.

Bouwmeester, R.J., Vlek, P.L., 1981. Rate control of ammonia volatilization from rice paddies. Atmos. Environ. 15, 131–140.

Corbin, R.A., Simpson, B.C., Anderson, M.J., Danielson, W.F., Field, J.G., Jones, T.E., Kincaid, C.T., 2005. Hanford soil Inventory Model Rev.1. CH2M Hill Hanford Group, Inc., Richland, WA.

Denham, M.E., Looney, B.B., 2005. Gas: a Neglected Phase in Remediation of Metals and

Radionuclides. Savannah River National Laboratory, Aiken, SC, pp. 1–23.

Dong, W., Ball, W.P., Liu, C., Wang, Z., Stone, A.T., Bai, J., Zachara, J.M., 2005. Influence of calcite and dissolved calcium on uranium (VI) sorption to a Hanford subsurface sediment. Environ. Sci. Technol. 39, 7949–7955.

Dong, W., Brooks, S.C., 2006. Determination of the formation constants of ternary complexes of uranyl and carbonate with alkaline earth metals (Mg^{2+}, Ca^{2+}, Sr^{2+}, and Ba^{2+}) using anion exchange method. Environ. Sci. Technol. 40, 4689–4695.

Dong, W., Tokunaga, T.K., Davis, J.A., Wan, J., 2012. Uranium(VI) adsorption and surface complexation modeling onto background sediments from the F-Area Savannah river site. Environ. Sci. Technol. 46, 1565–1571.

Dresel, P.E., Wellman, D.M., Cantrell, K.J., Truex, M.J., 2011. Review: technical and policy challenges in deep vadose zone remediation of metals and radionuclides. Environ. Sci. Technol. 45, 4207–4216.

Emerson, H.P., Di Pietro, S., Katsenovich, Y., Szecsody, J., 2017. Effects of ammonium on uranium partitioning and kaolinite mineral dissolution. J. Environ. Radioact. 167, 150–159.

Fox, P., Davis, J.A., Zachara, J.M., 2006. The effect of calcium on aqueous uranium(VI) speciation and adsorption to ferrihydrite and quartz. Geochem. Cosmochim. Acta 70, 1379–1387.

Heidmann, I., Christl, I., Leu, C., Kretzschmar, R., 2005. Competitive sorption of protons and metal cations onto kaolinite: experiments and modeling. J. Colloid Interface Sci. 282, 270–282.

Jackson, M.L., 1985. Soil Chemical Analysis - Advanced Course, second ed. Parallel Press, Madison, WI.

Katsenovich, Y.P., Cardona, C., Szecsody, J., Lagos, L.E., Tang, W., 2018. Assessment of calcium addition on the removal of U(VI) in the alkaline conditions created by NH_3 gas. Appl. Geochem. 92, 94–103.

Lagaly, G., Ziesmer, S., 2003. Colloid chemistry of clay minerals: the coagulation of montmorillonite dispersions. Adv. Colloid Interface Sci. 100, 105–128.

Mashal, K., Harsh, J.B., Flury, M., Felmy, A.R., Zhao, H., 2004. Colloid formation in Hanford sediments reacted with simulated tank waste. Environ. Sci. Technol. 38, 5750–5756.

McKinley, J.P., Zachara, J.M., Wan, J., McCready, D.E., Heald, S.M., 2007. Geochemical controls on contaminant uranium in vadose Hanford formation sediments at the 200 area and 300 area, Hanford Site, Washington. Vadose Zone J. 6, 1004–1017.

Morse, J.W., Arvidson, R.S., 2002. The dissolution kinetics of major sedimentary carbonate minerals. Earth Sci. Rev. 58, 51–84.

Morse, J.W., Mackenzie, F.T., 1990. Geochemistry of Sedimentary Carbonates. ElSevier, New York, NY.

Moyes, L.N., Parkman, R.H., Charnock, J.M., Vaughan, D.J., Livens, F.R., Hughes, C.R., Braithwaite, A., 2000. Uranium uptake from aqueous solution by interaction with goethite, lepidocrocite, muscovite, and mackinawite: an X-ray absorption spectroscopy study. Environ. Sci. Technol. 34, 1062–1068.

Powell, B.A., Kersting, A.B., Zavarin, M., Zhao, P., 2008. Development of a Composite Non-electrostatic Surface Complexation Model Describing Plutonium Sorption to Aluminosilicates. Lawrence Livermore National Laboratory LLNL-TR-408276.

Qafoku, N.P., Ainsworth, C.C., Szecsody, J.E., Bish, D.L., Young, J.S., McCready, D.E., Qafoku, O.S., 2003a. Aluminum effect on dissolution and precipitation under hyperalkaline conditions: II. Solid phase transformations. J. Environ. Qual. 32, 2364–2372.

Qafoku, N.P., Ainsworth, C.C., Szecsody, J.E., Qafoku, O.S., 2003b. Aluminum effect on dissolution and precipitation under hyperalkaline conditions. J. Environ. Qual. 32, 2354–2363.

Qafoku, N.P., Ainsworth, C.C., Szecsody, J.E., Qafoku, O.S., 2004. Transport-controlled kinetics of dissolution and precipitation in the sediments under alkaline and saline conditions. Geochem. Cosmochim. Acta 68, 2981–2995.

Qafoku, N.P., Icenhower, J.P., 2008. Interactions of aqueous U (VI) with soil minerals in slightly alkaline natural systems. Rev. Environ. Sci. Biotechnol. 7, 355–380.

Serne, R.J., Bjornstad, B.N., Horton, D.G., Lanigan, D.C., Lindenmeier, C.W., Lindberg, M.J., Clayton, R.E., LeGore, V.L., Orr, R.D., Kutnyakov, I.V., 2004. Characterization of Vadose Zone Sediments below the TX Tank Farm: Probe Holes C3830, C3831, C3832 and 299-W10-27. Pacific Northwest National Laboratory (PNNL), Richland, WA (US). Environmental Molecular Sciences Laboratory (EMSL).

Serne, R.J., Last, G.V., Gee, G.W., Schaef, H.T., Lanigan, D.C., Lindenmeier, C.W., Lindberg, M.J., Clayton, R.E., Legore, V.L., Orr, R.D., 2008. Characterization of Vadose Zone Sediment: Borehole 299-E33-45 Near BX-102 in the B-bx-by Waste Management Area. Pacific Northwest National Laboratory, Richland, WA.

Singandhupe, R.B., Rajput, R.K., 1989. Ammonia volatilization from rice fields in alkaline soil as influenced by soil moisture and nitrogen. J. Agric. Sci. 112, 185–190.

Szecsody, J.E., Cantrell, K.J., Krupka, K.M., Resch, C.T., Williams, M.D., Fruchter, J.S., 1998. Uranium Mobility during in Situ Redox Manipulation of the 100 Areas of the Hanford Site. Pacific Northwest National Laboratory, Richland, WA, pp. 41.

Szecsody, J.E., Truex, M.J., Qafoku, N.P., Wellman, D.M., Resch, T., Zhong, L.R., 2013. Influence of acidic and alkaline waste solution properties on uranium migration in subsurface sediments. J. Contam. Hydrol. 151, 155–175.

Szecsody, J.E., Truex, M.J., Zhong, L., Qafoku, N., Williams, M.D., McKinley, J.P., Wang, Z., Bargar, J., Faurie, D.K., Resch, C.T., 2010. Remediation of Uranium in the Hanford Vadose Zone Using Ammonia Gas: FY 2010 Laboratory-scale Experiments. Pacific Northwest National Laboratory (PNNL), Richland, WA (US). Environmental Molecular Sciences Laboratory (EMSL).

Szecsody, J.E., Truex, M.J., Zhong, M.J., Johnson, T.C., Qafoku, N.P., Williams, M.D., Greenwood, W.J., Wallin, E.L., Bargar, J.D., Faurie, D.K., 2012. Geochemical and geophysical changes during ammonia gas treatment of vadose zone sediments for uranium remediation. Vadose Zone J. 1–13.

Tokunaga, T.K., Wan, J.M., Pena, J., Sutton, S.R., Newville, M., 2004. Hexavalent uranium diffusion into soils from concentrated acidic and alkaline solutions. Environ. Sci. Technol. 38, 3056–3062.

Wan, J.M., Larsen, J.T., Tokunaga, T.K., Zheng, Z.P., 2004. pH neutralization and zonation in alkaline-saline tank waste plumes. Environ. Sci. Technol. 38, 1321–1329.

Wellman, D.M., Zachara, J.M., Liu, C., Qafoku, N.P., Smith, S.C., Forrester, S.W., 2008. Advective desorption of uranium(VI) from contaminated Hanford vadose zone sediments under saturated and unsaturated conditions. Vadose Zone J. 7, 1144–1159.

Zachara, J.M., Brown, C., Christensen, J., Davis, J.A., Dresel, E., Liu, C., Kelly, S., Mckinley, J., Serne, J., Um, W., 2007. A Site-wide Perspective on Uranium Geochemistry at the Hanford Site. Pacific Northwest National Laboratory, Hanford, WA.

Zavarin, M., Powell, B.A., Bourbin, M., Zhao, P., Kersting, A.B., 2012. Np(V) and Pu(v) ion exchange and surface-mediated reduction mechanisms on montmorillonite. Environ. Sci. Technol. 46, 2692–2698.

Zhao, H., Deng, Y., Harsh, J.B., Flury, M., Boyle, J.S., 2004. Alteration of kaolinite to cancrinite and sodalite by simulated Hanford tank waste and its impact on cesium retention. Clay Clay Miner. 52, 1–13.

Zheng, Z., Zhang, G., Wan, J., 2008. Reactive transport modeling of column experiments on the evolution of saline–alkaline waste solutions. J. Contam. Hydrol. 97, 42–54.

Zhong, L., Szecsody, J.E., Truex, M.J., Williams, M.D., Liu, Y., 2015. Ammonia gas transport and reactions in unsaturated sediments: implications for use as an amendment to immobilize inorganic contaminants. J. Hazard. Mater. 289, 118–129.